Conclusion

The takeovers of the 1980s, like those of the previous merger waves, partly reflect the desired expansion of large corporations in times of easy access to funds. With the current antitrust stance, this expansion has taken place within the areas of expertise of the acquiring firms and has made corporations more focused. Although the jury is still out on this takeover wave, the disappointing experience with conglomerates suggests that these takeovers are likely to raise efficiency as corporations realize the gains from specialization.

REFERENCES AND NOTES

1. G. S. Stigler, *Am. Econ. Rev.* **40**, 23 (1950).
2. D. C. Mueller's "The Effects of Conglomerate Mergers" [*J. Bank. Financ.* **1**, 315 (1977)] is a survey of these studies. D. J. Ravenscraft and F. M. Scherer's *Mergers, Sell-Offs, and Economic Efficiency* (Brookings Institution, Washington, DC, 1987) is the most recent and detailed study.
3. S. N. Kaplan and M. Weisbach, "Acquisitions and Divestitures: What Is Divested and How Much Does the Market Anticipate?" University of Chicago, mimeo, 1990.
4. S. Bhagat, A. Shleifer, R. W. Vishny, "Hostile Takeovers in the 1980s: The Return to Corporate Specialization," *Brookings Pap. Econ. Act. Microecon.* (1990), p. 1.
5. M. C. Jensen, *Har. Bus. Rev.* **67**, 61 (1989).
6. For a review of this evidence, see A. Shleifer and L. H. Summers, "The Noise Trader Approach to Finance" [*J. Econ. Perspect.* **4**, 19 (1990)].
7. F. R. Lichtenberg, "Industrial De-Diversification and Its Consequences for Productivity," Columbia University, manuscript, 1990.
8. H. Servaes, "Tobin's Q, Agency Costs, and Corporate Control," University of Chicago, mimeo, 1989.
9. R. Stillman, *J. Finan. Econ.* **11**, 225 (1983).
10. A. Shleifer and L. H. Summers, "Breach of Trust in Hostile Takeovers," in *Corporate Takeovers: Causes and Consequences*, A. J. Auerbach, Ed. (Univ. of Chicago Press, Chicago, 1988), pp. 33–68.
11. J. Rosett, "Do Union Wealth Concessions Explain Takeover Premiums? The Evidence on Contract Wages" (NBER Working Paper 3187, National Bureau of Economic Research, Cambridge, MA, November, 1989).
12. J. Pontiff, A. Shleifer, M. Weisbach, "Excess Pension Fund Reversions After Takeovers," University of Rochester, mimeo, 1989.
13. M. C. Jensen, *Am. Econ. Rev.* **76**, 323 (1986).
14. S. N. Kaplan, "The Effects of Management Buyouts on Operating Performance and Value," *J. Finan. Econ.* **24**, 217 (1989).
15. B. H. Hall, "The Impact of Corporate Restructuring on Industrial Research and Development," *Brookings Pap. Econ. Act. Microecon.*, p. 85 (1990).
16. M. L. Dertouzos, R. K. Lester, R. M. Solow, *Made in America* (MIT Press, Cambridge, MA, 1989).

Optical Matter: Crystallization and Binding in Intense Optical Fields

MICHAEL M. BURNS, JEAN-MARC FOURNIER, JENE A. GOLOVCHENKO

Properly fashioned electromagnetic fields coupled to microscopic dielectric objects can be used to create arrays of extended crystalline and noncrystalline structures. Organization can be achieved in two ways: In the first, dielectric matter is transported in direct response to the externally applied standing wave optical fields. In the second, the external optical fields induce interactions between dielectric objects that can also result in the creation of complex structures. In either case, these new ordered structures, whose existence depends on the presence of both light and polarizable matter, are referred to as *optical matter.*

EFFORTS TO ORGANIZE MATTER ON MICROSCOPIC SCALES are playing an increasingly important role in scientific and technological endeavors. Examples are the fabrication of electronic circuits, optical elements, and mechanical machines, as well as the synthesis and modification of the macromolecules central to modern chemistry and biology. At the submicroscopic scale there is an extraordinarily high degree of order in matter due to the natural proclivity of atoms to organize themselves into molecules and extended structures by electron bonding. Here we present a description and demonstration of methods of effecting the organization of matter on length scales characteristic of the wavelength of light, still microscopic but thousands of times the typical separation of atoms. This is accomplished by causing intense light beams to interact with matter under controlled conditions. In contrast to photographic and photolithographic methods which rely on slow chemical transformations, we are here concerned with the rapid organization, manipulation, and transport of matter directly with light.

Our work has been stimulated in part by the increase in understanding that has recently been achieved in the study of laser-induced forces on microscopic matter, and in part by the desire to manipulate and organize matter at length scales comparable with the wavelength of light. It hardly seems necessary to justify interest in this regime of distances today for researchers in disciplines ranging from modern biology to microelectronics and optics. We note however that 50 years ago Land (*1*) faced and solved the problem of orienting microscopic crystals in a lacquer to create the first artificial optical polarizers through various electro- and magneto-static, as well as mechanical forces. In a sense, the following article represents a continuation of that program although at a higher level of spatial organization and by new methods made available through laser technology.

Ashkin and co-workers have carried out pioneering experiments in the area of optical forces on small dielectric objects (*2–4*). These results on optical levitation, optical trapping, and material transport

M. M. Burns and J.-M. Fournier are at the Rowland Institute for Science, Cambridge, MA 02142. J. A. Golovchenko is at Harvard University, Cambridge, MA 02138, and the Rowland Institute.

in highly focused beams play a major role in our experiments. Ashkin's work has led to the development of new tools for cellular and intercellular biology (*5–9*), as well as extensions to the atomic scale with the exciting recent progress in laser trapping of atoms by Chu, Pritchard, Wieman, Phillips, and others (*10–13*).

Our work began with the goal of creating periodic crystals of micrometer size dielectric objects with micrometer size lattice constants. Yablonovitch (*14*) has proposed such structures for optical bandgap material with interesting properties, one of which is to serve as a cavity in which one can suppress spontaneous optical emission. We also envisioned the possibility of assembling arrays of microscopic biologically interesting cells and macromolecules, as well as optically and electronically active materials for other applications. Our idea was to organize such crystals by creating an optical standing wave pattern with a regular array of intensity antinodes at the positions where dielectric objects were ultimately desired. The standing waves would be produced in water containing micrometer-sized spheres which then organize themselves by occupying the periodic positions at the antinode maxima driven by the optical forces. This strategy has indeed been successful and we present a first account of this work here, stressing the formation of a variety of two-dimensional crystals, culminating in the demonstration of a current curiosity in solid-state physics, a quasi-crystal.

During the course of these crystallization studies we discovered that, in addition to the trapping forces imposed by the standing wave interference patterns, there were new induced interactions between spheres that we had not anticipated (*15*). We isolated and identified this new force which can cause binding between light-scattering objects. The second part of this paper concerns this binding force. Overall we seek to call attention to the fact that matter may be spatially organized at the length scale of light by both the trapping and binding phenomena. These light-matter structures we refer to as *optical matter*.

Experimental Setup

We begin with a discussion of the experimental methods and present the rather graphic results we have obtained in the study of induced crystallization in optical standing waves. The apparatus is schematically illustrated in Fig. 1. An argon ion laser delivering up to 10 W of power at a wavelength of 5145 Å supplies the incident light. This light beam is split and formed into multiple beams, whose intensities, polarizations, focal properties, and mutual phases are all carefully controlled, and brought to a common focus on a sample cell which contains the matter to be organized. The interfering light beams therein generate optical standing wave fields which serve as the templates by which order will be imposed. Three beams are shown converging on the sample cell in Fig. 1. In our optical crystallization experiments we have used as few as one and as many as five beams.

After passing through the sample cell, the transmitted light beams then serve the added purpose of providing a monitor of both the standing wave field and the condensed phases of optical matter that have accumulated. This is accomplished in two ways. In the first the transmitted light is collected in optics that constitutes a projection microscope which ultimately presents a real image on a screen for viewing and photographing. In the second method we directly view the angular distribution of the transmitted light with no additional optical elements. The formation of large arrays of ordered material in the cell causes strong diffraction of the incident light beams which can provide comprehensive quantitative information about both its static and dynamical properties.

The sample cell is simply a thin glass chamber containing a colloidal suspension of micrometer-sized polystyrene spheres in water. The spheres are dispersed in the liquid by ultrasonic shaking and by screening the monopolar charges on the spheres with a buffer salt dissolved in the water. Two fused silica plates, separated by 200 μm, make up the front (bottom) and back (top) surface of the cell, through which the light enters and exits, respectively. The cell is mounted so the plates are in the horizontal plane (with light entering from below) to minimize the adverse effects of convective liquid flow.

Figure 2 shows the images of various standing wave intensity fields at the back of the cell. The first is obtained by having only two incident beams converge on the sample (Fig. 2A). The spacing, D, between intensity maxima, which form long parallel planar optical traps, is given by

$$D = \frac{\lambda}{2\sin(\theta/2)} \quad (1)$$

where θ is the convergence angle between the incident beams and λ is the wavelength of the light. In this example D is 5 μm. Figure 2B shows a standing wave image obtained with three beams converging equiangularly on a sample cell without spheres. Rather than parallel planes running perpendicular to the front and rear faces of the cell, we now have a lattice of hexagonal rod-like intensity maxima extending through the cell, and we image the cross section at the back surface. Finally by relaxing the geometric requirement of equiangular convergence a lattice of elongated intensity maxima is achieved as illustrated in Fig. 2C.

From the principle of superposition the general form of the time-averaged spatial field intensity in the sample cell is a sum of the individual incident beam intensities plus a set of periodic interfer-

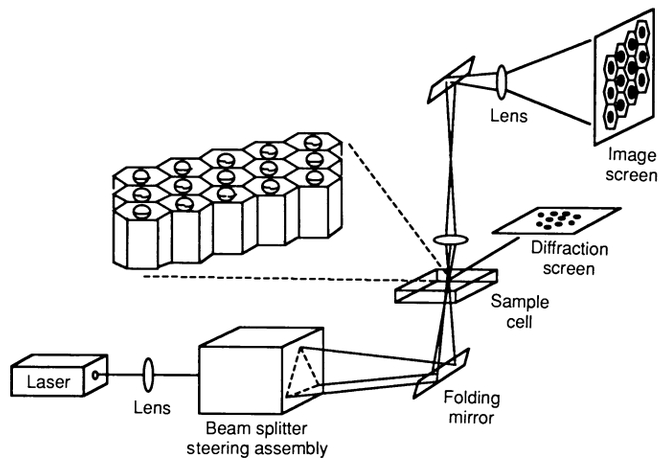

Fig. 1. Experimental setup for optical crystallization experiments.

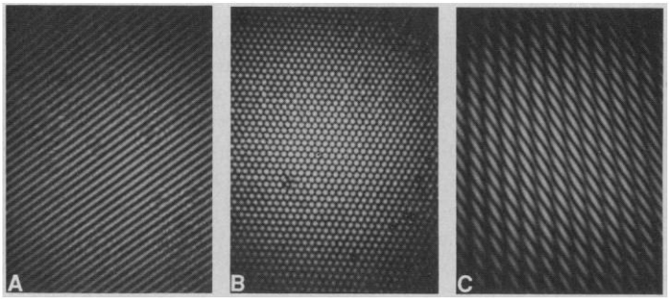

Fig. 2. Intensity patterns produced in sample cell (**A**) by two incident beams, (**B**) by three equiangular beams, and (**C**) by three non-equiangular beams.

ence terms which provide the intensity modulations shown in Fig. 2. The spatial periodicity of each interference term is determined by linear combinations of the (linearly independent) differences of incident wave vectors which form the reciprocal lattice basis for the real-space periodicities. If the required reciprocal lattice vectors are three or less and linearly independent, a periodic space lattice in intensity results. If there are more (perhaps because there are more than four incident beams) the real-space intensity distribution will, in general, be aperiodic with some interesting possibilities, as we shall see. Note that each interference term in the intensity sum will be multiplied by a factor dependent on the incident beam intensities and polarization and each will have a phase that depends on the relative phases of the incident beams (which are also experimentally adjustable parameters.)

Optical Forces

The mechanism by which dielectric matter may be trapped in optical standing waves ultimately derives from the most fundamental considerations of electromagnetism, which define the fields to be proportional to the forces they exert. How static or low-frequency forces on matter can result from the extremely high-frequency stimulation of optical fields merits discussion. From a microscopic view, the Lorentz force equation summarizes the most elementary aspect of the field-matter interaction. The Lorentz force on a body with a distribution of charge density $\rho(t)$ and current density $\mathbf{j}(t)$ in volume V immersed in electric and magnetic field strengths $\mathbf{E}$ and $\mathbf{B}$ is

$$\int (\rho(t)\mathbf{E}(t) + \mathbf{j}(t) \times \mathbf{B}(t))\, dV \tag{2}$$

Static forces on the body may result from the high-frequency undulations of $\mathbf{E}$ and $\mathbf{B}$ because $\rho(t)$ and $\mathbf{j}(t)$ will generally oscillate sympathetically in time with these fields. A time average of the Lorentz force over a cycle of the fields thus generally yields a net static component of force on the body. The simplest application of these ideas is to a system of a charge e bound to an oppositely charged central heavy mass to form an undamped harmonic oscillator of natural frequency ω_0. One then finds for the time averaged force

$$\mathbf{F} = \frac{1}{2}\alpha \nabla E^2, \quad \alpha = \frac{e^2}{m(\omega_0^2 - \omega^2)} \tag{3}$$

which can most conveniently be derived from a potential energy function

$$W = -\frac{1}{2}\alpha E^2 \tag{4}$$

where α is the oscillator polarizability at the optical frequency ω, and m is the mass of the oscillating bound charge (*16*). The validity of the above equations requires that the extension of the motion of the oscillator be smaller than the wavelength of light so that only the field at the center of the oscillator motion is needed in the formulas.

For macroscopically dense matter the formulation of the physics of forces is somewhat more involved (*17–24*), in part because the $\mathbf{E}$ and $\mathbf{B}$ fields that appear in Maxwell's equations in dense matter are now usually taken to be fields averaged over the atomic scale fluctuations of the system with the electromechanical degrees of freedom of the charges hidden in dielectric and magnetic response functions. In addition the elastic properties of the system play an important role and must be considered. It is possible in this description, at least at low enough frequencies and in the absence of dissipation, to deduce the reaction forces necessary to keep dielectric objects in spatial equilibrium from the principle of virtual work. Here the Maxwell stress tensor $\mathbf{T}$ plays a major role. For a sphere with dielectric permittivity ε_1 in a fluid of dielectric permittivity ε_2, the aforementioned force is given by

$$\mathbf{F} = \int_S \mathbf{T} \cdot \mathbf{n}\, ds \tag{5}$$

with

$$T_{ij} = \varepsilon_1 E_i E_j - \frac{\varepsilon_1}{2} E^2 \delta_{ij} + \frac{1}{\mu} B_i B_j - \frac{1}{2\mu} B^2 \delta_{ij} \tag{6}$$

where the integration surface, S, lies outside the sphere. The dependence on the sphere size and permittivity are contained implicitly in Eq. 5 in the fields, which are the total (incident plus scattered) fields. Using this formalism and perturbation theory for the scattered fields one finds for a small dielectric sphere of radius a

$$\mathbf{F} = \frac{1}{2} \frac{\varepsilon_1 - \varepsilon_2}{\frac{\varepsilon_1}{\varepsilon_2} + 2} a^3 \nabla E^2 \tag{7}$$

which is derivable from a potential energy function

$$W = -\frac{1}{2} \frac{\varepsilon_1 - \varepsilon_2}{\frac{\varepsilon_1}{\varepsilon_2} + 2} a^3 E^2 \tag{8}$$

One may estimate the effectiveness of the standing wave intensity modulations in trapping dielectric objects by comparing the minimum energy of interaction in Eq. 8 with the thermal energy kT. The latter has the value of 26 meV at room temperature and for our experiments the trap depths are of the order of electron volts when light power of several watts is focused down to areas of several hundred square micrometers. Under these conditions strong trapping in the vicinity of intensity maxima is expected, if there is also a mechanism for dissipating the sphere's kinetic energy. In our experiments this is supplied by the viscosity of the surrounding fluid.

Finally a few technical notes for specialists. First, the above formalism will not reproduce classical radiation pressure effects unless radiation damping effects are included in the dynamical equations of the fundamental charges in motion. Even off-resonance this leads to phase shifts in the charge motion, as well as the scattered fields. Through Eq. 2 or Eq. 5 these give rise to non-zero time averaged forces that are commonly identified with radiation pressure. Second, the evaluation of scattered fields for spheres as large as the wavelength of light requires more detailed calculations (*25*). However, when the index of the spheres is not too different from the fluid a perturbation-like Born approximation may be used as an estimate of the scattered fields. With these comments we end our discussion of the basic theory and return to experiment.

Optical Crystallization

When a dilute solution of the colloidal suspension of spheres is added to the cell, allowed to settle, and the laser beams are turned on, at first no spheres are seen in the projected image of the top of the cell. Over a period of a few seconds, the radiation pressure from the incident laser light lifts the spheres from the bottom to the top of the cell, where they collect at the positions of the intensity maxima of the standing wave field, and are imaged (along with the standing wave field) in the projection system.

Figure 3 shows images of "optical crystals," in this case two-dimensional lattices of microscopic spheres formed in the standing wave configurations of Fig. 2. The intensity maxima are clearly seen to act as a periodic array of optical traps. Although it cannot be

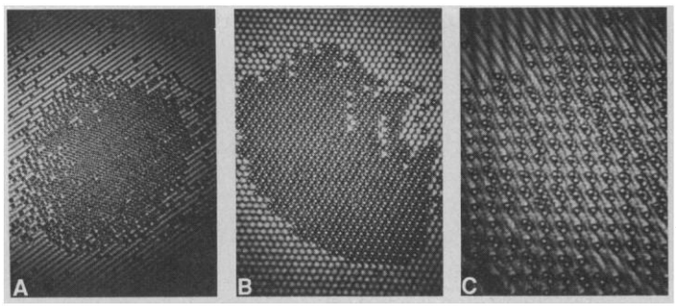

Fig. 3. Spheres (3.4 μm in diameter) distributed by the gradient force in the intensity patterns of Fig. 2.

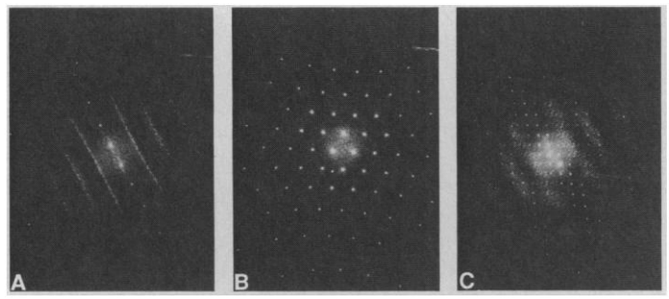

Fig. 4. Diffraction patterns formed by arrays of sphere in Fig. 3.

demonstrated through still photographs like those shown here, the spheres are in fact completely trapped in the various wells and make no transitions between them (unless the optical intensity is much reduced). It is however still possible to observe fluctuations of the sphere positions within each well due to thermally induced Brownian motion normally expected for such small objects suspended in a viscous fluid. The energy required to completely trap a sphere is just that required to overcome such thermal motion and hence depends on the temperature of the spheres and their surroundings.

In Fig. 3A long lines of spheres are induced, somewhat randomly distributed along the well length. In Fig. 3B only a single sphere fits in each of the symmetrically shaped periodic wells, while in Fig. 3C more than one sphere can fit in each well and a more complicated crystal basis can be formed.

It is possible to exercise additional control over the optical crystals demonstrated in Fig. 3 by jiggling the cell relative to the optical field so that hydrodynamic Stokes forces also act on the spheres. In this way one can create and anneal large rafts of nearly defect free optical crystals at the back of the cell. Induced Stokes forces from mechanical cell motion can also be used to measure the optical trap depths.

We have also induced crystals with periodicity perpendicular to the cell face by reflecting the light from the rear surface back into the cell. Such crystals are harder to image and are usually studied through Bragg diffraction; although we are continuing their study, we show no examples of them in this report. We have trapped titanium dioxide spheres and even *Escherichia coli* bacteria in our optical standing waves; we will report on this elsewhere.

Figure 4 shows the diffraction patterns obtained from the three crystalline configurations of Fig. 3. Figure 4A shows the diffraction pattern expected of a two-dimensional crystal melted along the direction perpendicular to the plane of the two incident light beams but highly ordered otherwise. In Fig. 4B, all of the disorder connected with the melted direction has disappeared and a two-dimensional diffraction pattern of sharp spots is obtained. Finally Fig. 4C shows the pattern obtained for the more complex crystal

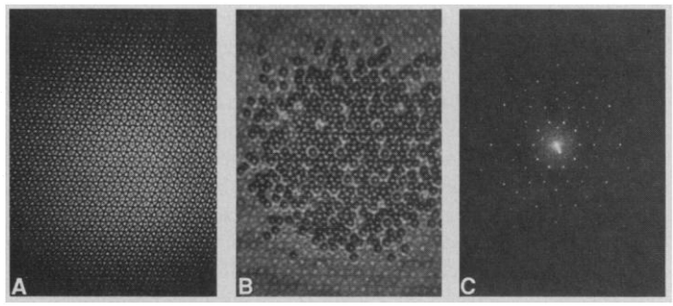

Fig. 5. (**A**) Intensity pattern formed by five equiangular beams, (**B**) the "quasicrystal" sphere assembly which results, and (**C**) the corresponding diffraction pattern.

that contains multiple spheres in a crystal unit cell. Clearly the presence of defects is not nearly as manifest as in the spatial image.

The last example of optical crystallization is intended to demonstrate that more elaborate structures than periodic arrays can be constructed. The standing wave pattern formed by five equiangular coherent beams yields the two-dimensional template of a structure, only recently discovered to exist in nature, called a "quasicrystal." These are structures that exhibit long-range quasiperiodic translational order and long-range orientational order but with disallowed (in this case fivefold) crystallographic symmetry (*26*). Figure 5A shows such a standing wave pattern. Note the high level of orientational order but lack of translational order in the structure. Figure 5B shows the array of trapped spheres, and Fig. 5C shows the diffraction pattern from that structure. This image has been recorded from the scattering of a single additional helium-neon laser beam to isolate the expected quasicrystal diffraction spots; a pattern obtained from the argon-ion laser beams is complicated by the superposition of five diffraction pictures with non-overlapping spots and is not shown here.

Optical Binding

Having established that the previously described forces were in accord with established theory, we were somewhat surprised to observe phenomena that fell outside the scope of the previous discussion. Curiously, these effects were first observed when only a single Gaussian beam 15 or 20 times larger than an individual sphere was focused on the sample cell. As expected, when spheres were added, one by one, to this large potential well, a close-packed crystal of spheres began to appear centered on the beam. After a few tens of spheres collected, strange crystal faceting and motion of individual spheres was noted as they first hit the top surface of the cell near the periphery and then moved toward the central close-packed crystal. It became clear to us that the individual spheres were not only being influenced by the incident beam but also by the beam scattered by the central crystal.

Indeed none of the commonly known forces between dipoles seemed able to account for the above observations. Standard Van der Waals energies of interaction are known to fall off at rates proportional to inverse seventh or sixth power of the dipole spatial separation depending on whether retardation is or is not important. Static permanent dipoles experience inverse cube interaction energies solely as a result of the static Coulombic forces between their constituents.

It does not seem to be well known, however, that the energy of interaction of two coherently optically induced dipole moments has the interesting and curious feature of depending on separation as only the inverse power of separation, multiplied by an oscillatory

factor such that the induced force between the dipoles changes sign every half wavelength of the exciting radiation field (*15*). It follows that such an interaction should result in the existence of optically induced, self-organized bound states of the two dipoles with stable separations every wavelength at the positions where the induced force is zero and the interaction energy a minimum.

Our most successful experiment to date demonstrating this previously undetected force is illustrated in Fig. 6. Now only a single beam is incident on the cell. The optical configuration has been changed to shape the incident beam into the form of a narrow ribbon at the back of the sample cell. The electric field vector is perpendicular to the long orientation of the ribbon, which is roughly 5 μm wide and several hundred micrometers across. One indeed sees spheres being captured into this long skinny trap. Once so captured, individual spheres can still move freely along the length of the trap. The density of spheres in solution is chosen so it is easy to obtain only two in the trap which may then be observed in isolation over a considerable period of time.

When the spheres are well separated in the trap their motion along the trap length appears random, characteristic of diffusive fluctuating trajectories in a dissipative fluid (Brownian motion). As two spheres approach one another they appear to spend excessive time in each others' company. A very effective and accurate method by which the relative motion of the spheres can be studied is through the diffraction patterns they create in the scattered field. Figure 7 shows the data from such a diffraction pattern extracted from one frame of a video tape of the diffraction screen during an extended trajectory of two spheres in the trap. From the recording one obtains such pictures every thirtieth of a second from which the sphere separation and trajectory can be calculated to an accuracy of a few hundred angstroms.

Figure 8 shows the time development of the relative separation deduced in this way for 1.41-μm spheres at the middle of the trap. The motion still exhibits random character due to Brownian motion yet there is a clear enhancement in the probability of finding the spheres at special distances separated from one another by a wavelength of light. The histogram projected on the right-hand side of the figure further illustrates the effect. There is also a peak at the smallest separation, determined by the size of the spheres.

It is possible to understand these observations with a simplified model in which an incident plane wave falls on a pair of optical scatterers which are completely characterized by their polarizabilities. In this case one can solve the coupled Maxwell-Lorentz-Newton equations (in the dipole approximation) for the self-consistent time-dependent dipole moments induced by the total optical field (both incident and scattered components) and the resulting interaction between the dipoles as a function of their separation.

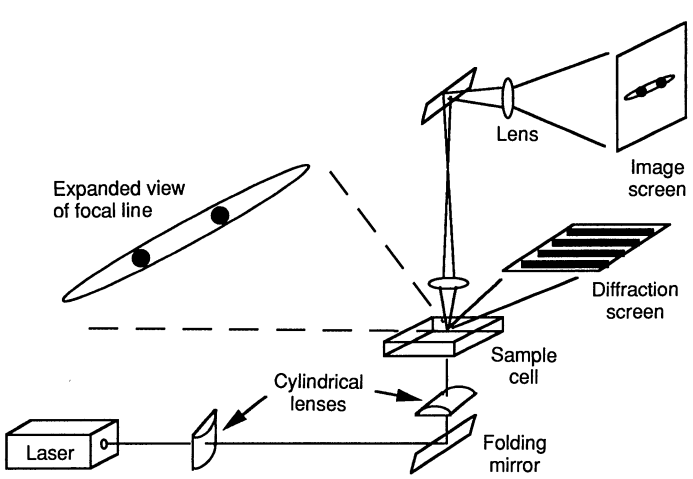

Fig. 6. Experimental setup for optical binding experiments.

Fig. 7. Cross section through intensity diffraction pattern of a pair of interacting spheres with the computer fit to that pattern.

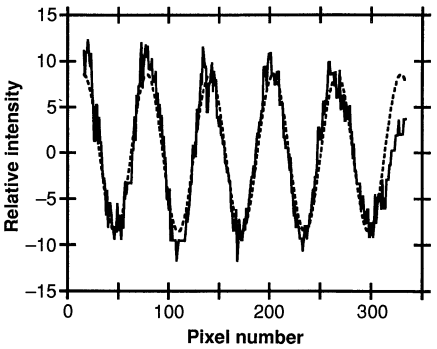

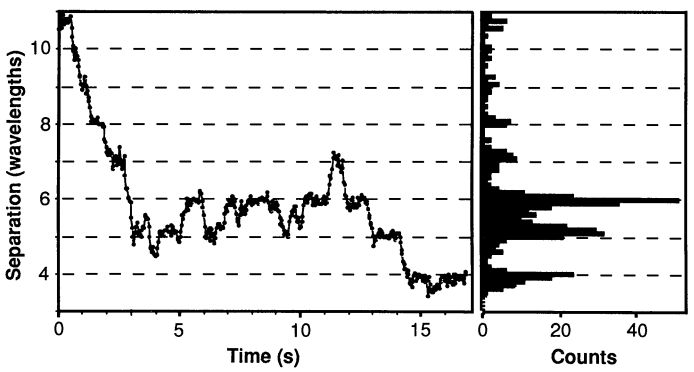

Fig. 8. Relative separation of two 1.43-μm-diameter spheres measured in units of wavelength of illuminating light in water. The plot on the left shows the time course of the separation, sampled at 1/30 second intervals, and the plot on the right is the corresponding histogram.

For the geometry of this experiment the physical origins of the optical binding forces are in this way seen to result from the time-averaged magnetic force from retarded radiation field current-current interactions. From the standpoint of an individual dipole, the forces originate from an interaction of the internal oscillator current with the light scattered from the neighboring dipole. The exchange of light energy between the scatterers plays a crucial role in the development of binding forces. Indeed the retardation between this scattered magnetic field and internal oscillator current allows a form of internal radiation pressure to develop whose sign depends on the separation of the dipoles. This sign variation with separation is the actual origin of the binding.

Quantitatively the above model predicts a potential energy of interaction given by (*15*)

$$W = -\frac{1}{2}\alpha^2\left(\frac{2\pi}{\lambda}\right)^2 \frac{\cos(2\pi r/\lambda)}{r} E^2 + O\left(\frac{1}{r^2}\right) \qquad (9)$$

The positions of minimum energy predicted by Eq. 9 are just at sphere separations, r, where the histogram in Fig. 8 shows experimentally the system is most likely to be found.

Of course our system does not consist of point dipoles, and a rigorous theoretical extension of our simple formula to the case of microscopic media has not yet been carried out. Nevertheless, we expect the overall features contained in Eq. 9 to be retained by more exact calculations which will hopefully be available soon. Those features that must remain are the periodic bound state positions, the long range of the interaction and the curious fact that the resultant time-averaged forces are not screened out even by a high direct-current conductivity of the fluid.

Optical Matter

Having demonstrated two extreme ways that light beams influence structure in the previous sections, we suggest that such organized systems can be considered a new form of matter. In contradistinction to ordinary "electronic matter" which is essentially organized and held together by the exchange of electrons between its constituents, this "optical matter" is organized and held together by photons. The forces generated by the light are quite different from those generated by electrons in ordinary matter—for example, the optical forces demonstrated here can be both extraordinarily long range, and periodic in space.

Optical matter, particularly for condensed extended systems, represents an especially interesting field of study because the optically induced interaction forces are amenable to continuous external control, both in intensity and geometry. Unlike ordinary matter in which this control is not available, in optical matter we have the opportunity to design and engineer structures using these new degrees of freedom. Diffractive optical elements and binary optics (*27, 28*) is ideally suited to the problem of crafting arbitrary intensity patterns to serve as templates of organization. In addition the scattered light between the constituents contributes its own organizing force. With only a single unstructured incident beam, systems can organize themselves into structures whose details will depend on the character as well as number of scatterers. We are currently investigating theoretically and experimentally just what such ground states might be, and what form excited states take. The consequences of these internal forces for organized structures are not obvious.

We can speculate about the uses of this optical matter. The statistical mechanics of such structures will surely provide a wealth of material for future experimental and theoretical research; in particular the large degree of control ought to aid in exploring and understanding system phase transitions. Already some interesting work has been done with ionic colloidal crystals (*29, 30*), and the extension to include optical forces seems exciting.

Yablonovitch's suggestion of optical bandgaps for periodic dielectrics has been mentioned; the techniques of this article show how such a controllable periodic array can be constructed. The decay of a single oscillator in a bandgap may indeed be inhibited, but what happens when a large number of such oscillators are coupled together—what sort of cooperative radiative behavior might be observed?

We envision the development of efficient means for converting optical matter into structures that are stable in the absence of a sustaining light field by in situ freezing, hardening, or curing the fluid medium. We also believe that preliminary translational and orientational ordering of microscopic biological materials in optical fields could be followed by order maintaining mechanical collection and concentration for structural studies with shorter length probes (such as x-rays).

Finally, atoms are the ultimate dielectric constituents. Many of the atomic traps recently demonstrated in fact depend on optical forces near resonance to confine and cool atoms. In these traps, atoms and ions are already observed to exhibit complicated behavior due to collective effects (*31–34*). It will be interesting to see how a near-resonant optical binding force can be realized for atoms, and whether similar control of crystal structures of atoms may be achieved.

In conclusion, we hope we have demonstrated some of the new and diverse ways that light beams may serve to organize matter on the microscopic scale. There will undoubtedly be further developments in this field as the study of more complex structures and multiple interactions are combined in future research. Practical applications resulting from this line of research may be expected to have increasing impact as we continue to acquire and require manipulative power over the microscopic environment around us.

REFERENCES AND NOTES

1. E. H. Land, *J. Opt. Soc. Am.* **41**, 957 (1951).
2. A. Ashkin, *Phys. Rev. Lett.* **24**, 156 (1970).
3. _____ and J. M. Dziedzic, *Science* **187**, 1073 (1975).
4. A. Ashkin, *ibid.* **210**, 1081 (1980).
5. _____ and J. M. Dziedzic, *ibid.* **235**, 1517 (1987).
6. _____, T. Yamane, *Nature* **330**, 769 (1987).
7. S. M. Block, D. F. Blair, H. C. Berg, *ibid.* **338**, 514 (1989).
8. M. W. Berns *et al.*, *Proc. Natl. Acad. Sci. U.S.A.* **86**, 4539 (1989).
9. A. Ashkin and J. M. Dziedzic, *ibid.*, p. 7914.
10. D. E. Pritchard, E. L. Raab, V. Bagnato, C. E. Wieman, R. N. Watts, *Phys. Rev. Lett.* **57**, 310 (1986).
11. S. Chu, J. E. Bjorkholm, A. Ashkin, A. Cable, *ibid.*, p. 314.
12. E. L. Raab, M. Prentiss, A. Cable, S. Chu, D. E. Pritchard, *ibid.* **59**, 2631 (1987).
13. P. L. Gould *et al.*, *ibid.* **60**, 788 (1988).
14. E. Yablonovitch, *ibid.* **58**, 2059 (1987); _____ and T. J. Gmitter, *ibid.* **63**, 1950 (1989).
15. M. M. Burns, J. M. Fournier, J. A. Golovchenko, *ibid.* **63**, 1233 (1989).
16. From Eqs. 3 and 4 onward we rely on the reader's perspicacity to recognize time-averaged quantities such as E^2.
17. J. A. Stratton, *Electromagnetic Theory* (McGraw-Hill, New York, 1940).
18. J. D. Jackson, *Classical Electrodynamics* (Wiley, New York, ed. 2, 1975).
19. L. D. Landau, E. M. Lifshitz, L. P. Pitaevskii, *Electrodynamics of Continuous Media* (Pergamon, Oxford, ed. 2, 1984).
20. J. P. Gordon, *Phys. Rev. A* **8**, 14 (1973).
21. H. A. Haus and J. R. Melcher, *Electromagnetic Fields and Energy* (Prentice-Hall, New Jersey, 1989).
22. P. Penfield, Jr., and H. A. Haus, *Electrodynamics of Moving Media* (MIT Press, Cambridge, 1967).
23. F. N. H. Robinson, *Phys. Rep.* **16C**, 314 (1975).
24. I. Brevik, *ibid.* **52**, 133 (1979).
25. J. P. Barton, D. R. Alexander, S. A. Schaub, *J. Appl. Phys.* **66**, 4594 (1989).
26. P. J. Steinhardt and S. Ostlund, Eds., *The Physics of Quasicrystals* (World Scientific, Singapore, 1987).
27. G. J. Swanson and W. B. Veldkamp, *Opt. Eng.* **28**, 605 (1989).
28. J. R. Leger, G. J. Swanson, W. B. Veldkamp, *Appl. Opt.* **26**, 4391 (1987).
29. N. A. Clark, A. J. Hurd, B. J. Ackerson, *Nature* **281**, 57 (1979); A. Chowdhury, B. J. Ackerson, N. A. Clark, *Phys. Rev. Lett.* **55**, 833 (1985).
30. C.Murray and D. H. Van Winkle, *Phys. Rev. Lett.* **58**, 1200 (1987).
31. T. Walker, D. Sesko, C. Wieman, *ibid.* **64**, 408 (1990).
32. F. Diedrich, E. Peik, J. M. Chen, W. Quint, H. Walther, *ibid.* **59**, 2931 (1987).
33. D. J. Wineland, J. C. Bergquist, W. M. Itano, J. J. Bollinger, C. H. Manney, *ibid.*, p. 2935.
34. S. L. Gilbert, J. J. Bollinger, D. J. Wineland, *ibid.* **60**, 2022 (1987).

35. We dedicate this paper to Edwin H. Land whose enthusiasm and encouragement inspired this work. We thank E. M. Purcell, N. Bloembergen, and A. Ashkin for useful discussions and criticism, and L. Hau, H. Xu, and M. Barillot for assistance with calculations and experiments. This work was carried out under the auspices of the Rowland Institute for Science.